Hot deformation studies on discontinuously reinforced Ti-Alloys

C. POLETTI[1*], S. KREMMER[2], H.P. DEGISCHER[1]

1 Vienna University of Technology. Karlsplatz 13 / E308 A-1040 Vienna, Austria
2 BÖHLER Schmiedetechnik GmbH & CoKG, Mariazellerstrasse 25 A-8605 Kapfenberg, Austria.
*Tel: +43-1-58801-30813. E-mail: cpoletti@mail.zserv.tuwien.ac.at

Abstract

Titanium alloys exhibit high specific strength and stiffness that fit structural applications demanding lightweight. The microstructure of the alpha-beta titanium alloys can be changed by thermomechanical processes such as heat treatments and pre-forging to achieve a certain ductility. Ceramic reinforcements can improve specific strength and stiffness, and also the wear resistance. In Situ particle reinforcement introduces neither further anisotropy to titanium alloys nor large internal stresses. The particulate reinforced titanium alloys (PRTi) are cheaper than the fiber reinforced materials and can be hot deformed.

The present work-studies the effect of thermomechanical processes on the microstructure of the PRTi produced in-situ by powder metallurgy from Ti-6Al-4V-powders with additions of 1.0%wt of B and 0.1%wt of C. In the as received material TiB is precipitated as needle like reinforcement in the Ti-6Al-4V-0.1C matrix. Hot compression tests on this PRTi and on conventional Ti64 (pre-deformed) were carried out between 850 and 1100°C at strain rates between 0.001 and 10/s using a servohydraulic Gleeble® device. The stability of the alpha and beta phases and of the TiB precipitates was studied by heat treatments before deformation. The beta transus temperature of the composite increases with respect to that of the Ti64 matrix indicating changes in composition. The microstructures before and after deformation were studied by SEM and light microscopy. Some broken particles are found in the deformed samples at lower and some porosity in the matrix at higher temperatures, respectively. These results are compared with those of TiC-particle reinforced Ti64 produced by Cold-Hot Isostatic Pressing (CHIP).

Keywords: Hot compression, TiB reinforcement, particulate reinfoced titanium, Ti64, damage.

1 Introduction

Titanium alloys are attractive for the aerospace, automotive and naval industries, as well as for medical applications. The advantages are the high specific mechanical properties up to high temperatures and the good corrosion resistance [1,2].

Ceramic reinforcement can further improve some of these properties [3]. The specific moduli of the composites are markedly higher than for the unreinforced materials. An increase in strength at room temperature was observed in previous works with different particulate reinforced titanium composites [4,5]. On the other hand, an important disadvantage of the composite is the lower ductility than that of conventional titanium alloys [6,7]. The ceramic reinforcements can be fibers, monofilaments, particles or whiskers.

Compared to the fiber reinforced titanium, the particulate reinforced titanium alloys (PRTi) are cheaper, can be forged, formed and have isotropic properties. The ceramics can be added to the matrix or can precipitate and grow within the alloy by addition of the desired precursors. The in-situ prepared metal matrix composites produce less internal stresses than the traditional metal matrix composites produced by mixing.

TiB and TiC are usually chosen for the production of particulate and whisker reinforced PRTi due to their high modulus, good thermal and chemical stability, low solid solubility and α coefficient of thermal expansion (CTE) similar to the matrix CTE [8]. This last characteristic reduces the concentration of internal stresses compared to other reinforcements such as SiC and B_4C.

The objective of this work is to study the deformation behavior at high temperatures of the in-situ composite Ti-6Al-4V-1.0B-0.1C produced by powder metallurgy. The potential hot workability of this material makes it interesting for forging and forming processes.

The results are compared to those obtained for Ti64 unreinforced and reinforced with 12%vol of TiC particles, both produced by powder metallurgy by Dynamet.

2 Experimental

The material investigated was Ti-6Al-4V-1.0B-0.1C (Ti64/TiB) produced by Cold-Hot Isostatic Pressing (CHIPing). Ti64 alloy and the B and C precursors were mixed to obtain an in-situ TiB particulate composite. To compare the flow behavior and the microstructural aspects, Ti-6Al-4V (Ti64) and Ti-6Al-4V reinforced with 12%vol of TiC particles (Ti64/TiC/12p) produced by CHIPing by Dynamet were also studied. Cylindrical samples of 10 mm diameter and 15 mm in length were fabricated for compression tests by erosion.

Compression tests at 850, 900, 950, 1010, 1050 and 1100°C and at 0.001-0.01-0.1 and $1s^{-1}$ were performed using a Gleeble®1500 machine, and a Gleeble®3600 was used at the same deformation temperatures and 10 s^{-1}. The samples were heated at 10K/s, and after holding at deformation temperature

during 2 minutes were deformed. The compression systems work with a servo-hydraulic mechanism, which deforms the sample during an electrical heating by the ohmic resistance of the material to a desired strain at a desired strain rate. The strain rate is constant during the experiment. The temperature was measured using a K-type thermocouple welded directly to the sample. In order to reduce the oxidation of the machine and of the sample, the tests were carried out under argon atmosphere at low pressure. To reduce the barreling of the sample as a consequence of the temperature gradient and the friction, "sandwiches" of graphite foil, colloidal graphite and Mo foil were used between the sample and the anvils (Figure 1). Due to the non-uniform deformation, transverse strain measurements (C-Gauge) were applied instead of the classic longitudinal strain measurement.

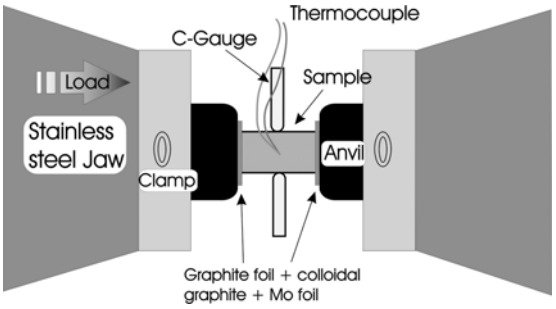

Figure 1. Gleeble arrangement for compression tests showing the welded thermocouple, the C-Gauge measurement system and the lubricant "sandwiches".

For measurements at $10s^{-1}$ strain rate a system of mechanical brakes was used to substitute the servohydraulic braking in order to obtain a constant strain rate during the test. After deformation, the samples were air-cooled. Compression tests at 850 and 950°C and $0.015\text{-}0.15\text{-}1.4s^{-1}$ were carried out with Ti64 and Ti64/TiC/12p. After deformation, the samples were water quenched.

The deformed specimens were cut through their axis parallel to the direction of compression, embedded, and finally ground and polished for metallographic investigations. The two phases of the Ti-6Al-4V alloy (α = hcp and β = bcc) were distinguished using the Back Scattered Electron (BSE) mode in a Philips 30XL Scanning Electron Microscope (SEM). The contrast observed is provoked by the distribution of the alloying elements: Al-rich α-phase dark, and V-rich β-phase bright. The TiB and TiC particles are darker (less dense) than the α phase. Light Optical Microscopy (LOM) was used after etching the samples with a Kroll solution to reveal the prior beta grains.

Heat treatments were carried out for Ti64/TiB in an inductive furnace under Ar atmosphere during 2, 10 and 60 minutes and at 850-900-950-1010-1050 and at 1100°C during 60 minutes and 1150°C during 2 and 10 minutes to study the stability of the microstructure before compression. After water quenching, the samples were prepared for metallography. Finally, quantitative analysis of SEM pictures of these samples was executed by means of AxioVision software. α/β ratio as well as the shape factor of the TiB particles were measured. The shape factor is defined as the ratio of the major to the minor dimension of a particle. (0 for a perfect circle shape and 1 for an ideal line). The TiB particles were divided into those smaller than 2 μm^2 and those bigger than $2\mu m^2$.

3 Results and discussion

3.1 Material.

For Ti64/TiB, it can be considered that all the B and C reacts with Ti to form TiB and TiC respectively, which results in 3%vol of TiB and 0.15%vol TiC. Thus, TiC cannot be identified using SEM and EDX.

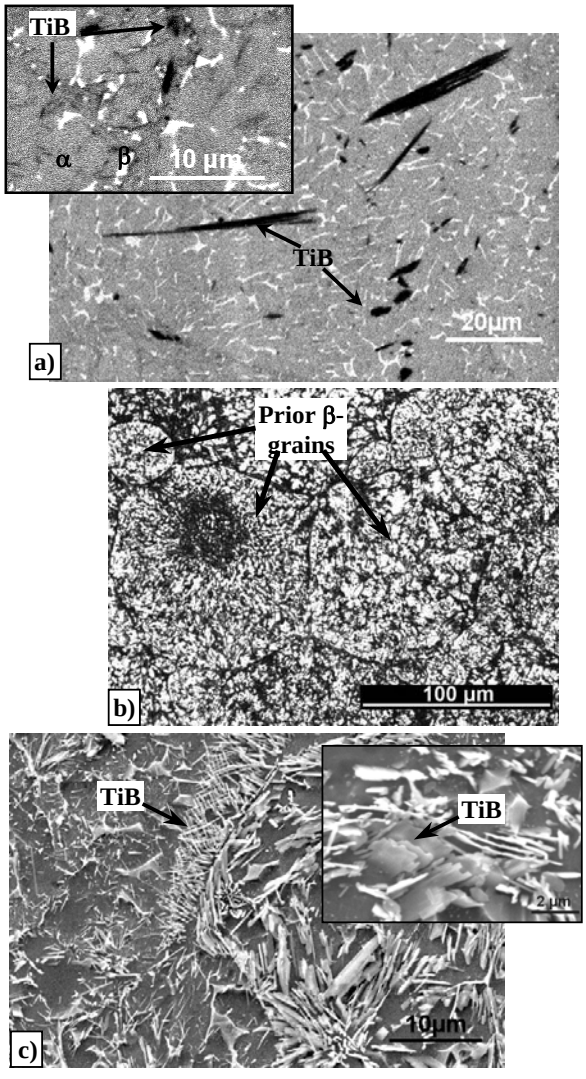

Figure 2. As received Ti64/TiB showing a) the TiB primary particles and needles (black) and the α–β phases (SEM) b) the prior β-grains (LOM) after etching and c) the TiB needles and platelets at the grain boundaries after etching (SEM)

The microstructure of the Ti64/TiB as received samples is shown in Figure 2. Using BSE mode it is possible to distinguish in black the TiB precipitates, in white the β-phase and in dark gray the α-phase. The matrix of the composite shows a fine globular α microstructure. Two types of TiB particles can be observed: big isolated particles between 5 and 40 μm length and 1-5 μm thick and small thin precipitates of 1-5μm length appearing in a needle shape.

Figure 2b) shows rounded prior β-grains, which remain from the Ti64 original powders. The TiB distribution, shape and size are different for different prior β-grain. Fine needles and plates of TiB can be found piled up at the grain boundaries (Figure 2c)).

Figure 3 shows the microstructure of the matrix of Ti64 (a) and the Ti64/TiC/12p (b). In both cases, lamellar α microstructure can be observed, as well as pores. TiC particles (in black) are decorating the prior β-grain boundaries in the composite. In contrast to this, the TiB reinforcement of Ti64/TiB grown in-situ (Figure 2) is more homogeneously distributed inside the prior β-grains provoking a better refinement of the α-phase.

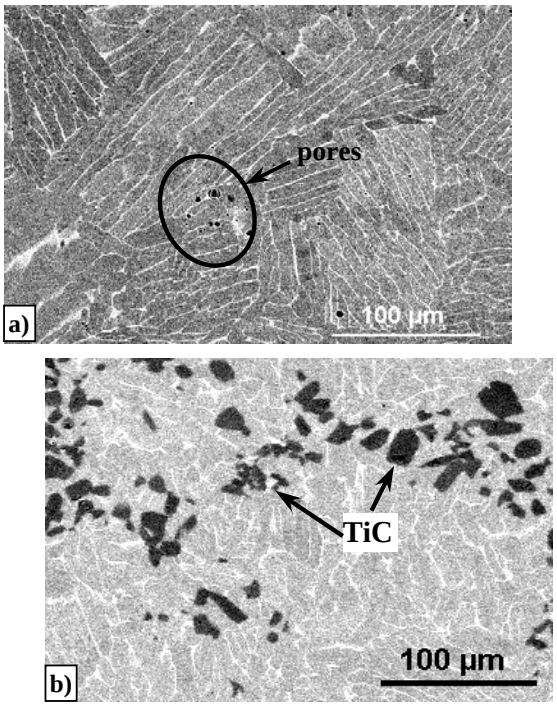

Figure 3. a) Ti64 unreinforced and b) Ti64 reinforced with 12%vol of TiC particles produced by powder metallurgy showing refined α-lamellae with TiC particles decorating the powder grain boundaries.

3.2 Heat treatments.

In the quantitative analysis (Figure 4) as well as in the micrographs (Figure 5) it is observed, that an increase of the temperature provokes an increment of the β-content, but neither changes in the TiB morphology nor in its distribution.

Figure 4 shows the β content in %vol with the temperature for different holding times determined by quantitative analysis. If extrapolated to 100% β-phase, the β-transus is around 1110°C, approximately 100°C higher than for commercial Ti64 [9]. This effect of C and B as alpha stabilizer in the matrix was also observed in previous works [10].

The micrographs show that the α–β transformation occurs inhomogeneously, depending on the prior β-grain, thus on the original TiB distribution. Primary α-phase can be observed up to 1100°C (Figure 5e). The increase of the beta transus temperature can be attributed to the dissolution of B in the matrix (less than 0.02%), and also to the stabilization of the alpha-phase due to the dissolution of C in the matrix up to 0.04% [11]. Furthermore, the work of Tamirisakandala et. al. [12] proposed that the rapid solidifications of the powders of titanium reinforced with TiB provokes the super-saturation of the solid solution before consolidation.

Furthermore, some V was found in the TiB platelets using EDX, according to the work of Bilous et. al [13]. This results in less V in the matrix, which means less beta stabilization.

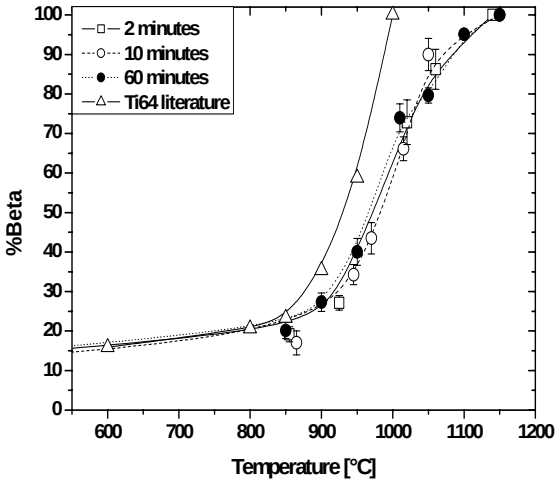

Figure 4. β vol % with increasing temperature after 2, 10 and 60 minutes holding time. The estimated β-transus is 1110°C.

The quantitative analysis shown also that the small TiB particles have a particle shape of 0.7±0.1 and the big ones 0.35 ±0.1, indicating small-elongated and big-rounded particles for all the temperatures and holding times of the heat treatments.

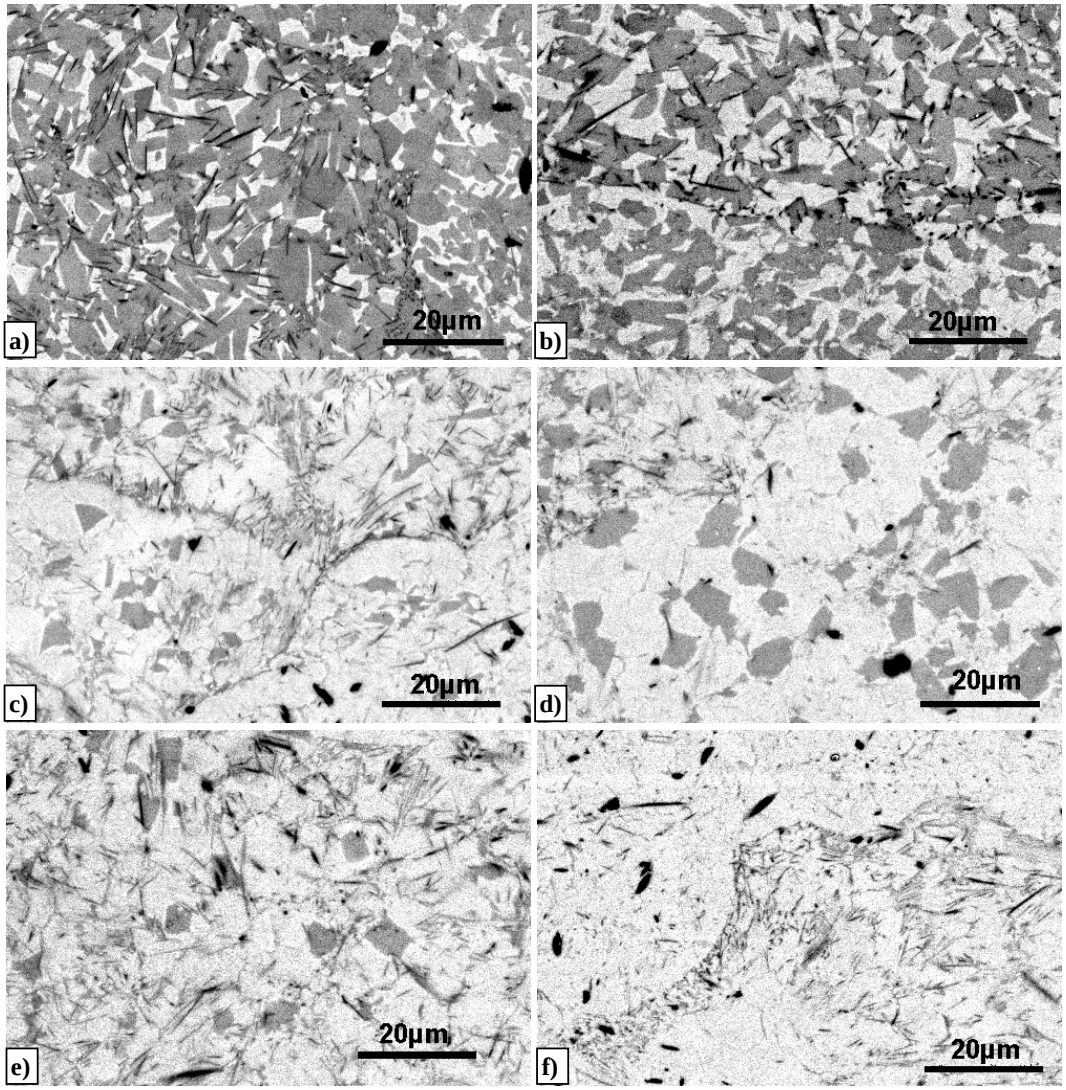

Figure 5. Microstructure after heat treatments, showing the alpha-beta transformation: white the β-phase, dark gray the α-phase and black the TiB particles a) 865°C 10 minutes: 17% β-phase, b) 950°C 60 minutes: 40% β-phase c) 1060°C 10 minutes: 89% β-phase d) 1050°C 60 minutes 80% β-phase, e) 1100°C 60 minutes: 95% β-phase, f) 1160°C 10 minutes: 100% β-phase

3.3 Deformation behavior

Figure 6 shows the flow curves at two different strain rates for the temperature range between 850 and 1100°C. The flow stresses increase with increasing strain rate and decreasing temperature. Softening, steady state and flow oscillations can be observed in the whole strain rate range [14]. Steady state occurs at high temperatures in the whole strain rate range, while oscillations and softening are characteristic for the deformation at lower temperatures.

In Figure 7 the flow curves at 850 and 950°C and at 0.015 and $1.4s^{-1}$ strain rate are shown for Ti64/TiC/12p and Ti64. An increase of the hot compressive stress of about 65-50% is provoked by the addition of 12%TiC particles to the Ti64 matrix. Flow softening is very similar for all three materials. The flow curves at 850 and 950°C of Ti64/TiB are also shown. At low strain rate, the behavior of the composite reinforced with TiB and unreinforced is the same, while an increase in the stress of about 15 and 35% at 950 and 850°C, respectively was observed at high strain rate. The flow softening is related to the damage produced in the lamellar microstructure at the triple grain boundary (wedge cracking), as well as at the particles in the case of the composites.

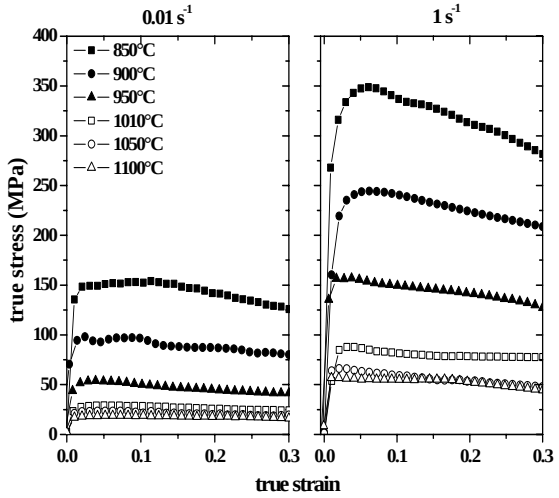

Figure 6. Ti64/TiB flow curves at 850-1100°C: a) 0.01 s^{-1} and b) 1s^{-1} showing a strong influence of the strain rate on the stress values

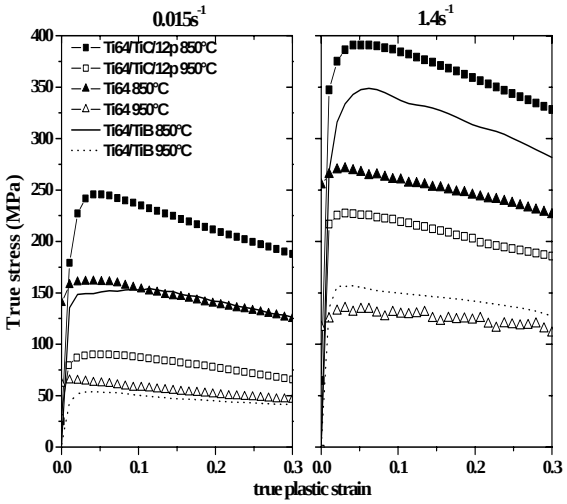

Figure 7. Flow curves at 850 and 950°C of Ti64/TiC/12p and Ti64 compared with those of Ti64/TiB (Figure 6) at a) 0.015s^{-1} and b) 1.4s^{-1} of strain rate showing similar softening but higher stress values for the composite with TiC particles.

Figure 8 shows the strain rate versus the stress in a double logarithmic scale for a total true strain of 0.05. From this figure, the stress exponent values n were calculated at each temperature as:

$$\dot{\varepsilon} = K\sigma^n \qquad \textbf{Equation 1}$$

where $\dot{\varepsilon}$ is the strain rate, σ the stress and K is a constant. Such a diagram looks similar for strains up to 0.3. It can be divided into two deformation regions: higher n values at high strain rates and n around 4 below 0.1s^{-1}. This is shown in Figure 9. At high strain rates (between 0.1 and 10s^{-1}) the n values >4 decrease with increasing temperature. The high n-values at high strain rates indicate power law breakdown, the earlier the lower the temperature. At low strain rates (between 0.001 and 0.1s^{-1}) n is approximately 4 and is independent of the temperature, which is in accordance with the power law creep exponent found in the work of Kawabata et. al. [15].

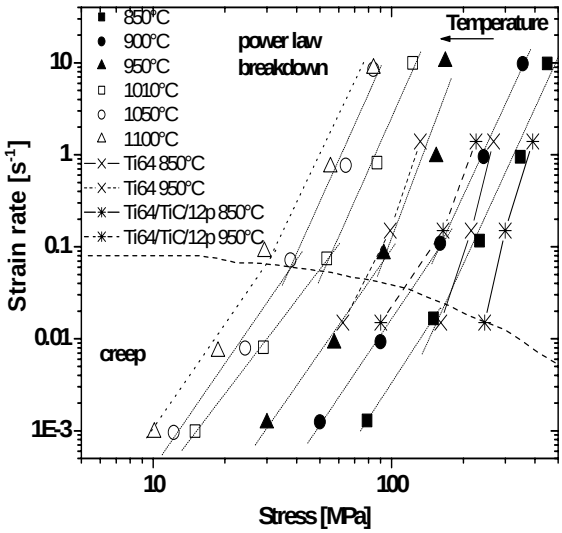

Figure 8. Strain rate vs. stress at different temperatures showing two deformation behaviors for each temperature at 0.05 true strain for all the materials tested.

In Figure 8, the values of strain rate vs. stress for Ti64 and Ti64/TiC/12p are also plotted for 850 and 950°C. For these materials the region of n ≈ 4 at 850°C is expected below 0.01s^{-1}.

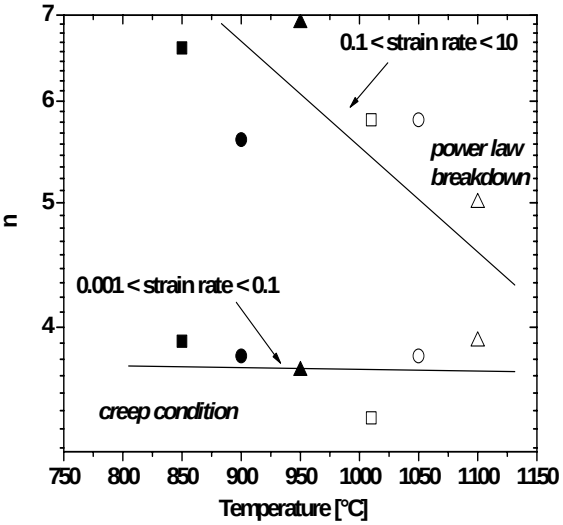

Figure 9. n values at low and high strain rates with the temperature for Ti64/TiB

The apparent energy of activation of the deformation process Q can be determined from:

$$\dot{\varepsilon} = A\sigma^n e^{-Q/RT} \qquad \textbf{Equation 2}$$

in the range of 0.001 to 0.1s^{-1} of strain rate, where A is a constant, R the gas constant, and T the absolute temperature.

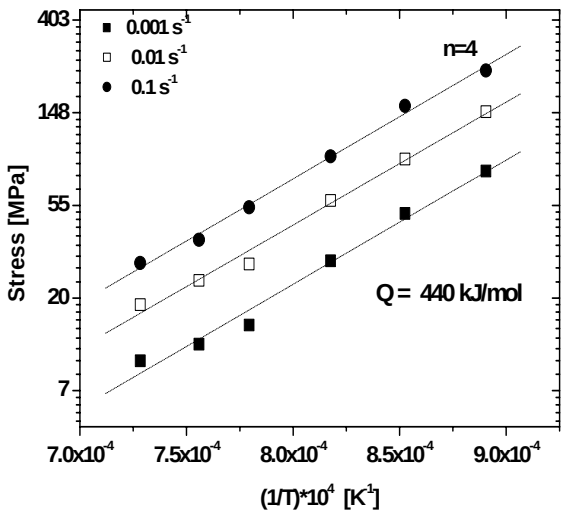

Figure 10. Apparent energy of activation for the range of 0.001 and 0.1s^{-1} of strain rate for Ti64/TiB material.

From Figure 10, the apparent energy of activation Q for Ti64/TiB is estimated to be around 440kJ/mol. This energy is much higher than that reported for self-diffusion in the alpha phase (150kJ/mol) [16], and higher than that one reported for Ti64 equiaxed [17] (330kJ/mol) in the alpha-beta range. The increase of the apparent energy of activation was also observed by F. Ma et. al [18] as a result of the addition of ceramic particles to the Ti-1100 alloy. As the energy of activation is increased by the alpha content, the increase of the beta transus temperature can increase the energy of activation in the $\alpha+\beta$ field. The Ti64/TiB and the unreinforced Ti64 present similar flow behavior at low strain rates, where the deformation mechanism is governed by diffusion in the alpha phase. At high strain rates, diffusion in Ti64 and its composites is too slow to produce the appropriate straining. Conservative strain hardening mechanisms become effective. The material is loaded beyond the creep regime, which can be related to the power law break down. Ti64/TiB produces significant hardening by the dispersions of the small size class TiB and by smaller grain size with respect to its matrix with lamellae α.

Ti64/TiC contains 12%vol particles, which increase the multiplication of dislocations during plastic deformation resulting in high strain hardening.

4 Microstructure after compression

The microstructure after deformation of Ti64/TiB is shown in Figure 11.

At low strain rates, pores in the matrix were found, while cracks in the particles and pores were formed at high strain rates.

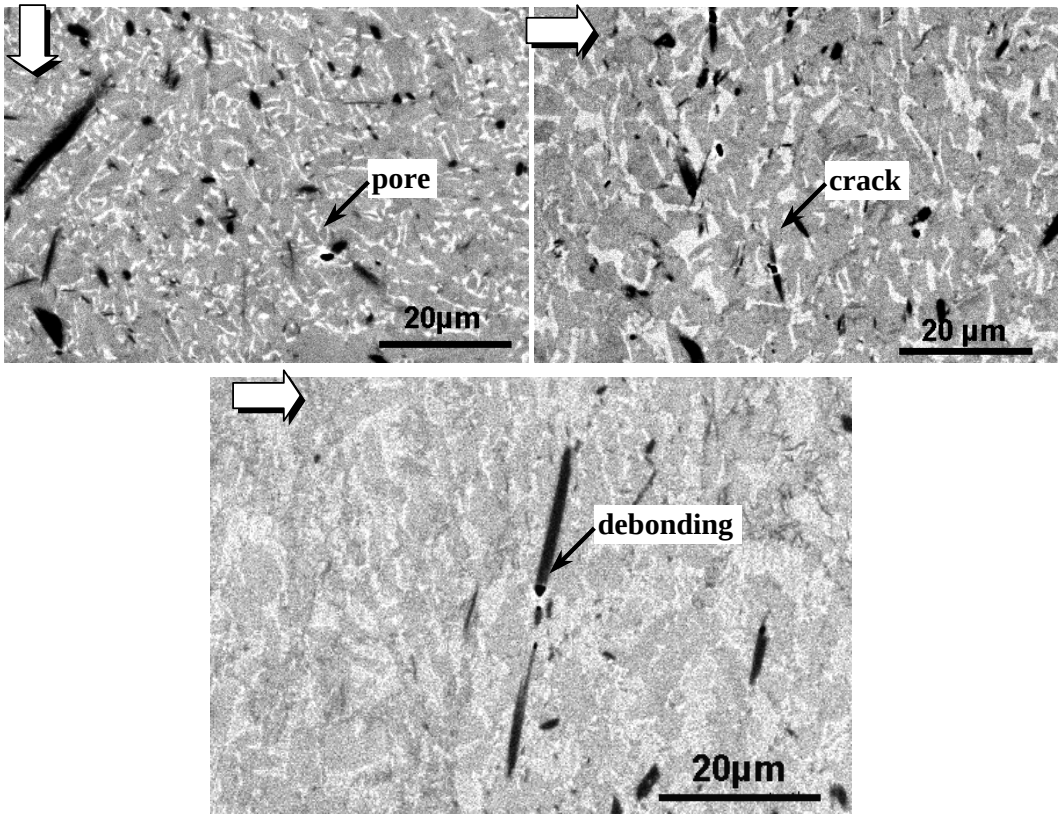

Figure 11. a) 850°C 0.001s^{-1}: pores in the matrix, b) 850°C 1s^{-1}: pores and cracks in the TiB particles c) 950°C 1s^{-1}: debonding of TiB particles. The white arrows show the direction of compression.

At high strain rates, the pores near the TiB particles are at the end of the big TiB "fibers". The strengthening mechanism of these elongated particles seems to be similar to that of short fibers in discontinuously reinforced metals, but the volume of less than 3% certainly is sub critical to produce significant stress partitioning. Finally, the small precipitates also reinforce the material by pinning the dislocations.

Figure 12 shows the microstructure after deformation up to 0.3 of true strain and water quenching of Ti64 and Ti64/TiC/12p. Porosity is higher than in the Ti64/TiB samples. At high strain rates, the pores in the matrix are observed preferentially at the triple beta-grain boundary, while at low strain rates the pores form in the soft beta phase. Debonding of TiC particles and cracks can be observed at low and high strain rates, respectively.

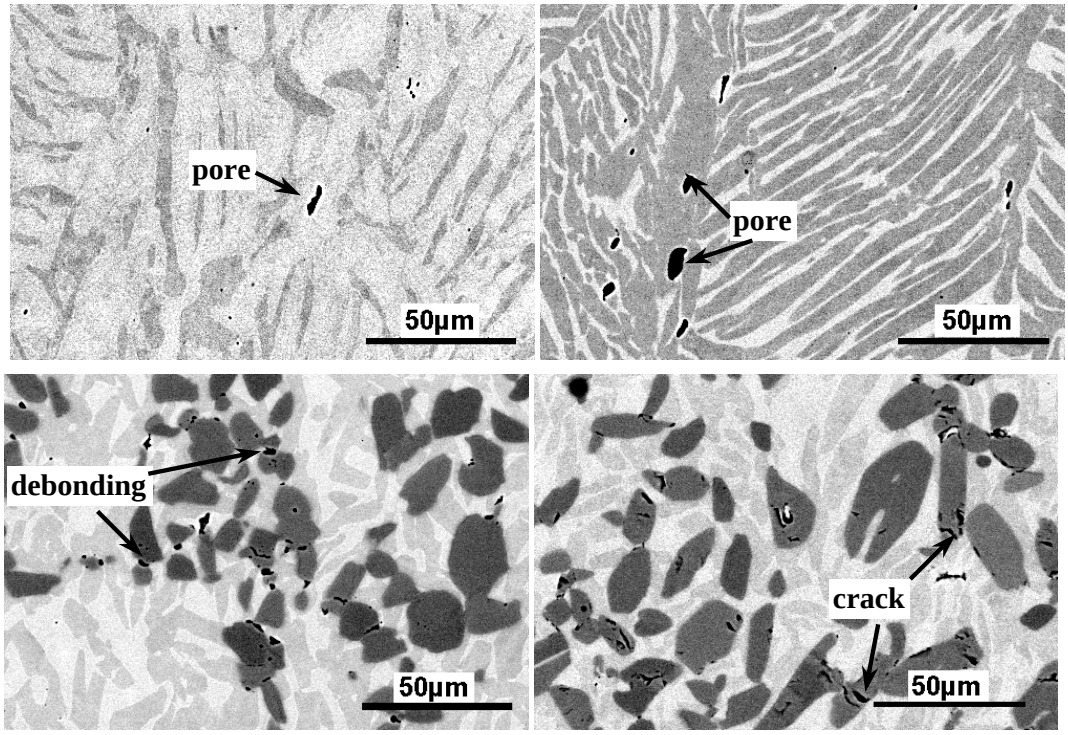

Figure 12 Samples after compression at 0.3 of true strain a) Ti64 at 950°C and 0.015s^{-1}: pores in the beta phase b) Ti64 at 850°C and 1.4s^{-1}: pores at the triple beta prior grain boundary c) Ti64/TiC/12p at 950°C and 0.015s^{-1}: debonding of the TiC particles and d) Ti64/TiC/12p at 950°C and 0.15s^{-1}: cracks at the TiC clusters.

5 Conclusions

An increment on the beta transus temperature of about 100°C with respect to the matrix was observed for the composite reinforced with TiB. The whole range of test temperatures is below β-transus for this composite. The results are compared with those of Ti64 and Ti64/TiC/12p in the α+β range as well.

Two mechanisms of hot compression were found for the Ti64/TiB material:

- At strain rates between 0.001 and 0.1s^{-1}, thermally activated deformation mechanisms prevail yielding a stress exponent around 4, with an apparent energy of diffusion of about 440kJ/mol.
- At strain rates between 0.1 and 10s^{-1}, power law breakdown occurs, and the dislocation mobility becomes more and more conservative, where the small TiB whiskers act like dispersion strengthening.
- Strain hardening is counteracted by damage resulting in softening above 0.05 true strain.
- Damage in the Ti64 lamellar microstructure and in the TiC reinforced Ti64 is enhanced due to higher strain concentrations compared to the fine globular microstructure of the Ti64/TiB composite.

6 Acknowledgments

The authors would like to thank to Dr. Mayer (Inst. of Materials Science and Technology.- Tech University Berlin) for the compression tests at high strain rates. The work is partially supported by the Federal Ministry of Economics and Labor in the framework of the Austrian Aeronautic Research (AAR) network

7 References

[1] Luo Guozhen, Zhen Quanpu and Deng Ju. Titanium ’95. III, 2704. **1995.**

[2] M. Peters, C. Leyens: Titan und Titanlegierungen, Wiley VCH, Weinheim **2002.**

[3] D.E. Alman, J.A. Hawk. Wear. 225-229.629 **1999.**

[4] Radhaskirshna B. Bhat, Seshacharyulu Tamirisakandala, Dale J. McEldowney, Daniel B. Miracle. In press. **2003.**

[5] C.Poletti, W. Marketz, H.P Degischer. Ti-2003 Science and Technology. Vol IV. 2531-2538. **2003**

[6] T. J. A. Doe1, P. Bowen. Composites Part A 27A 655-665. **1996**

[7] S. Qin, C. Chen, G. Zhang, W. Wang, Z. Wang. Materials Science and Engineering A272. 363–370. **1999**

[8] T.M.T. Godfrey, P.S. Goodwin, C.M. Ward-Close. Titanium '99. Proceedings of the ninth world conference of titanium. Pages 1868-1877. **1999**.

[9] M. Peters, C. Leyens: Titan und Titanlegierungen, Wiley VCH, Weinheim **2002**.

[10] S. Tamirisakandala, R.B. Bhat, D.B. Miracle, S. Boddapati, R. Bordia, R. Vanover, V.K. Vasudevan. Scripta Materialia 53. 217–222. **2005**

[11] K. Frisk. Computer Coupling of Phase Diagrams and Thermochemistry 27. 367–373. **2003**

[12] S. Tamirisakandala, R.B. Bhat, D.B. Miracle, S. Boddapati, R. Bordia, R. Vanover and V.K. Vasudevan. Scripta Materialia. Vol 53, Iss 2. 217-222. **2005**

[13] O.O. Bilous, L.V. Artyukh, A.A. Bondar, T.Ya. Velikanova, M.P. Burka, M.P. Brodnikovskyi, O.S. Fomichov, N.I. Tsyganenko and S.O. Firstov. Materials Science and Engineering: A, Vol 402, Iss 1-2. 76-83. **2005**

[14] C. Poletti, S. Kremmer. 12th European Conference on Composite Materials Proceedings **2006**. ***In Press***

[15] K. Kawabata, E. Sato, K. Kuribayashi. Scripta Materialia 50. 523–527. **2004.8**

[16] F. Dyment and C.M. Libanati. J. Mater. Sci. 3. 349–359. **1968**

[17] T. Seshacharyulu, S. C. Medeiros, W. G. Frazier, Y. V. R. K. Prasad.

[18] F. Ma, W. Lu, J. Qin, D. Zhang. Volume 60, Issue 3. 400-405. **2006**

Hot deformation studies on discontinuously reinforced Ti-Alloys

C. POLETTI[1], S. KREMMER[2], H.P. DEGISCHER[1]

1 Vienna University of Technology. Vienna, Austria
2 BOHLER Schmiedetechnik GmbH & CoKG. Kapfenberg, Austria.

Titanium 2006. San Diego, California

Contents

- Introduction
- Experimental
  - * Materials
  - * Compression tests
  - * Metallography. Quantitative analysis
- Results and discussion
  - * As received microstructures
  - * Heat treatments
  - * Deformation behavior
  - * Microstructures after compression
  - * Kinetic study
- Conclusions

Introduction

Titanium alloys: high specific mechanical properties up to high temperatures and good corrosion resistance.

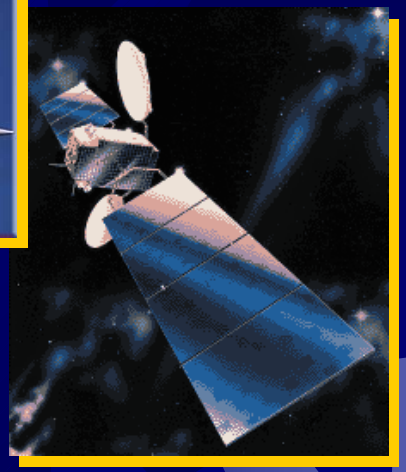

Ceramic reinforcement can further improve mechanical properties, increasing the specific moduli and strength at room temperature, by lowering the ductility. Ceramic reinforcements: fibers, monofilaments, particles or whiskers; in-situ or added.

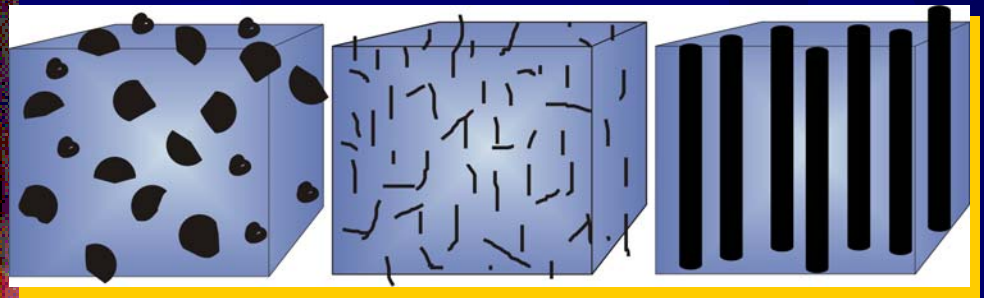

Particle short fibers monofilaments or long fibers

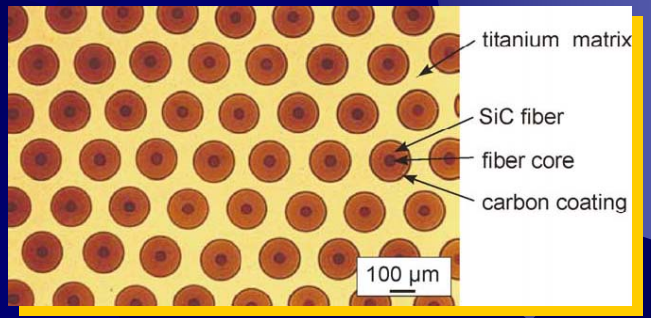

Introduction

TiB and TiC are chosen for particulate and whisker reinforcement

Objectives:

- Study the deformation behavior at high temperatures of the in-situ composite Ti-6Al-4V-1.0B-0.1C produced by powder metallurgy.

- Results compared to those obtained for Ti64 unreinforced and reinforced with 12%vol of TiC particles produced by powder metallurgy.

	Young's modulus (GPa)	CTE (x $10^{-6}K^{-1}$)	Stability at sintering temperature
Ti 64	115	8.8	n.a.
TiB	550	8.6	Very high
TiC	460	7.4	High
TiN	250	9.3	High
SiC	420	4.3	Very low: formation of TiC_x, Ti_5Si_3 and $Ti_5Si_3C_x$
Si_3N_4	320	3.2	Very low: consumption of particles and formation of Ti_5Si_3 and Ti_3Si
TiB_2	529	6.4	Medium: $Ti+TiB_2$ → TiB
B_4C	449	4.5	Low
Al_2O_3	350	8.1	Low: formation of $TiAl_3$

Introduction

Ti-6Al-4V-1.0B-0.1C
Ti64 powders + B and C. TiB and TiC particles grew *in-situ*

Ti64/TiC/12p
Ti64 powders + TiC ceramic particles. Dynamet

CHIPing process

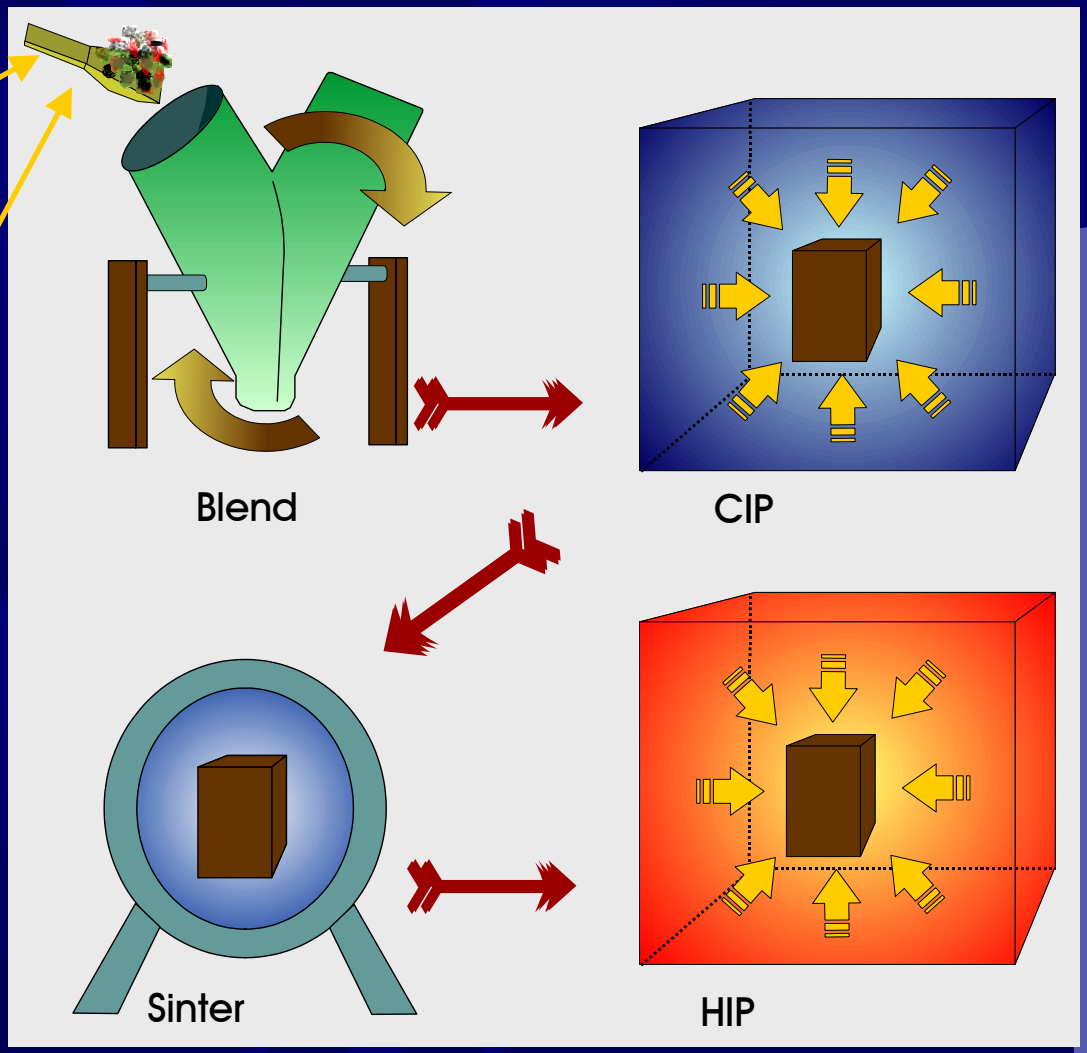

Experimental

Materials: Ti-6Al-4V-1.0B-0.1C (*Ti64/TiB*) produced by Cold-Hot Isostatic Pressing (CHIPing). For comparison: Ti-6Al-4V (*Ti64*) and Ti-6Al-4V reinforced with 12% vol of TiC particles (*Ti64/TiC/12p*).

Compression tests: with Gleeble®1500 and 3600 machines, 850-1100°C and 0.001-10s^{-1}.

Servo-hydraulic mechanism: to achieve constant strain rate. Electrical heating through the sample.

Temperature measurement: K-thermocouple.

Atmosphere: argon at low pressure.

Lubricant: "Sandwich" of graphite foil, colloidal graphite and Mo foil between the sample and the anvil.

Strain measurements: Transverse (C-Gauge)

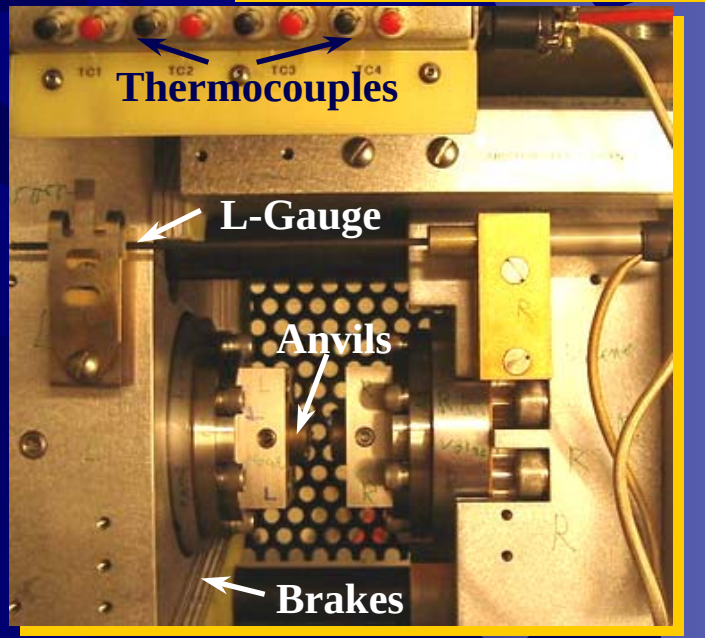

Experimental

Quantitative analysis:

Layers generation

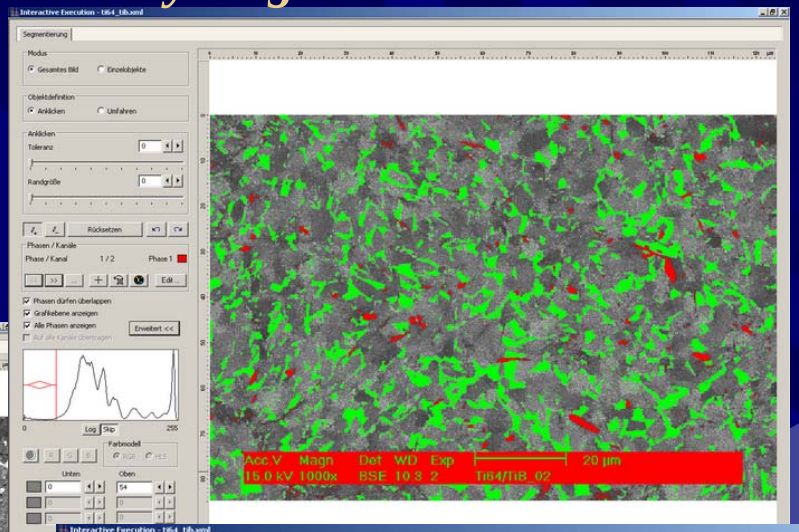

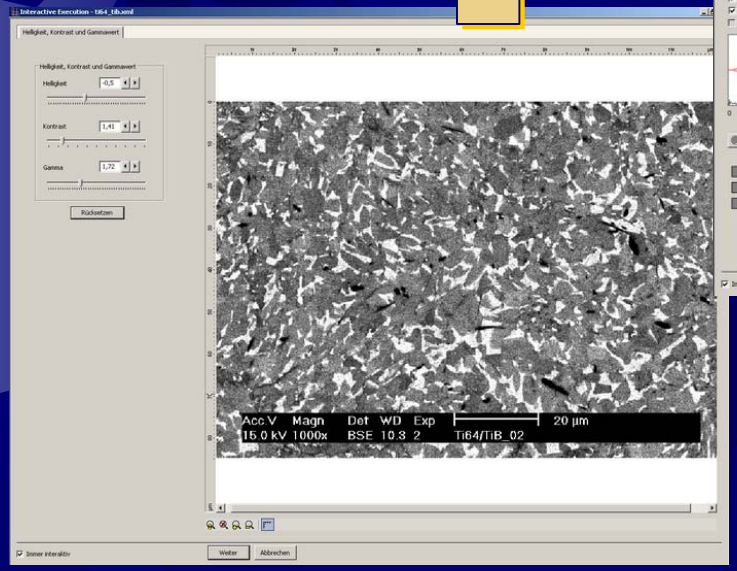

Image treatment

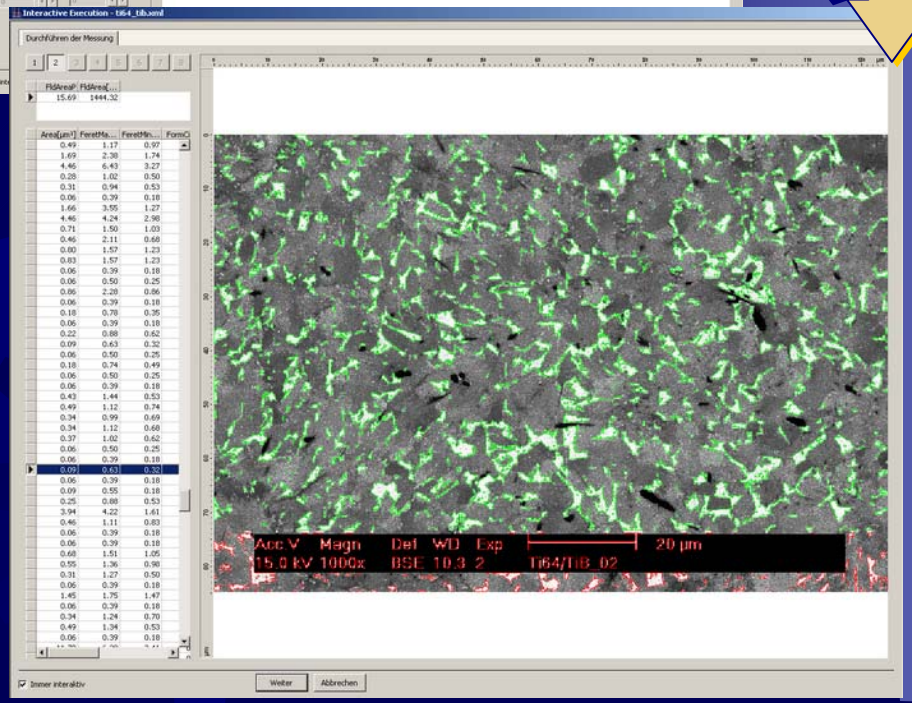

Results

Results. Microstructures.

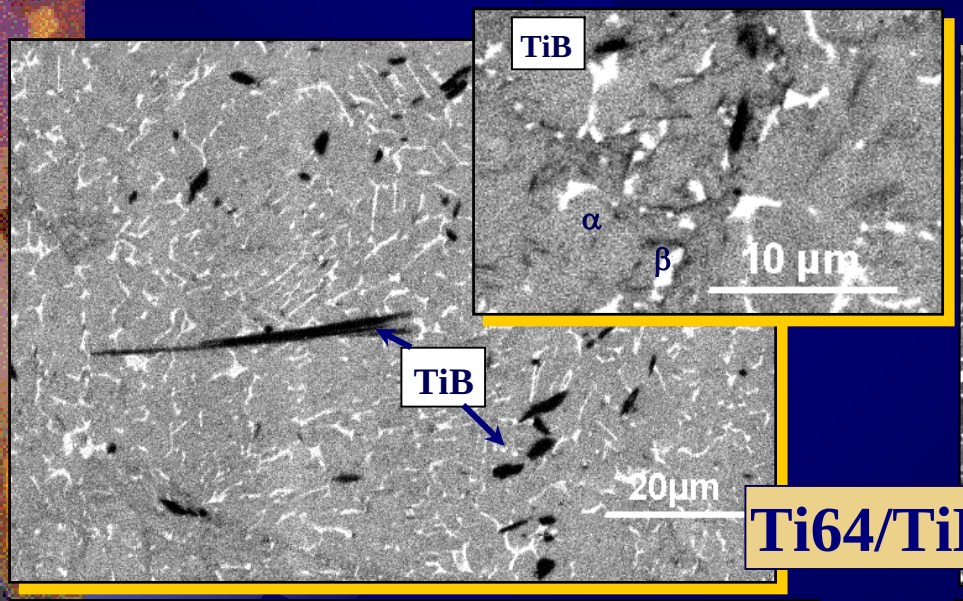

Ti64/TiB

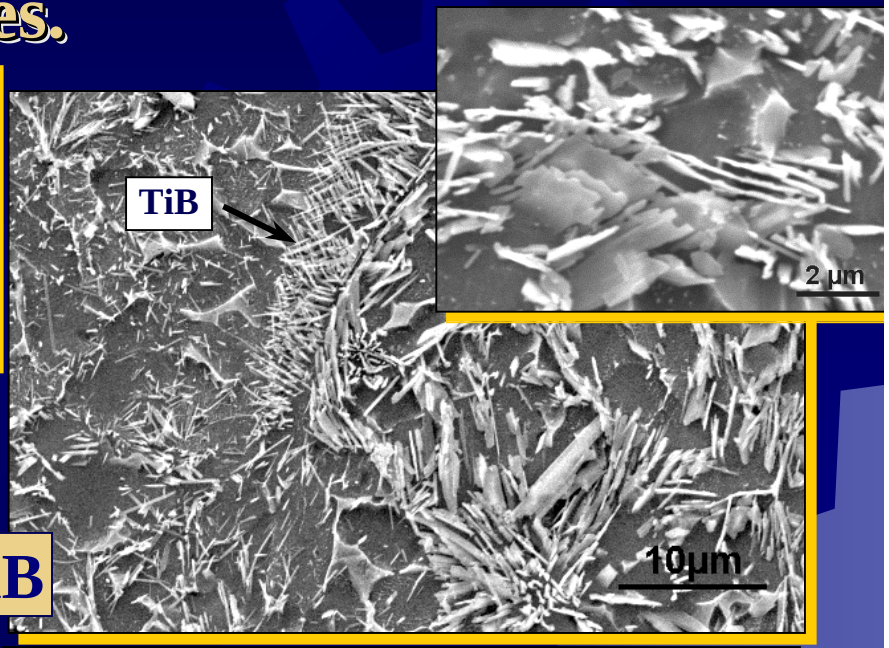

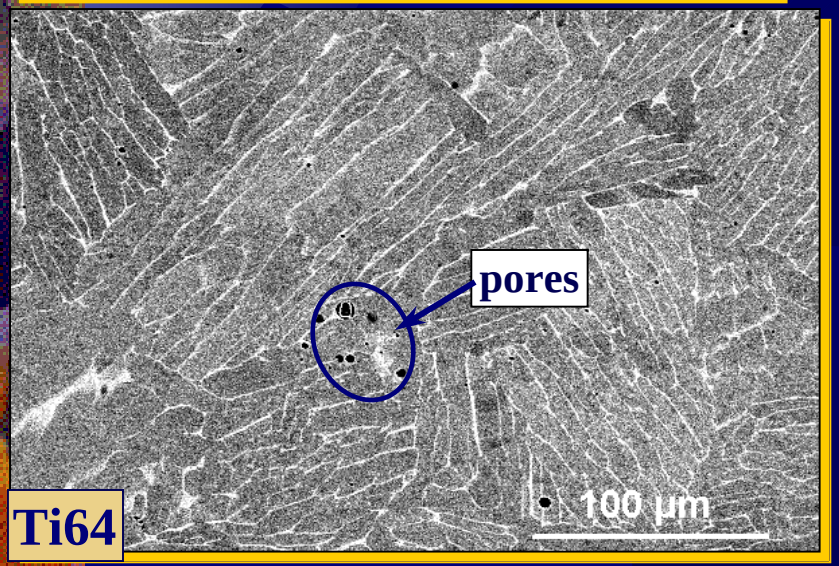

Ti64

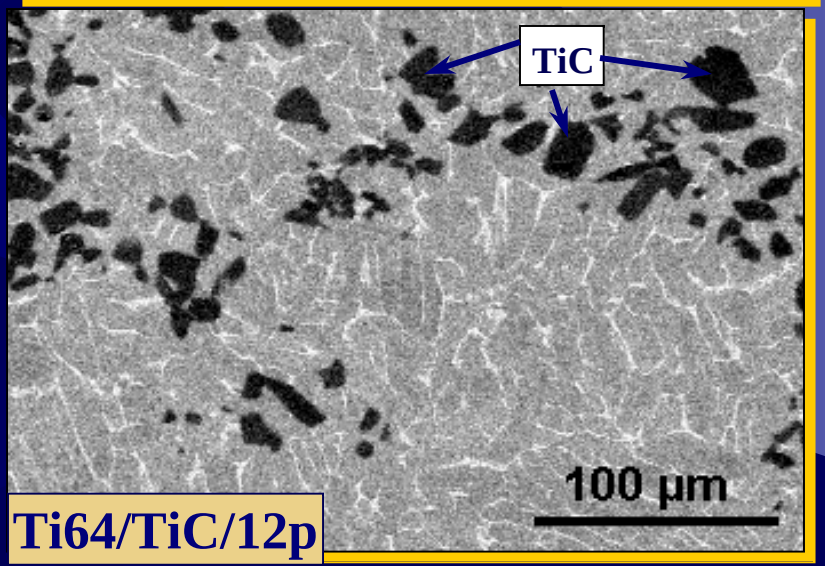

Ti64/TiC/12p

Results. Heat treatments of Ti64/TiB

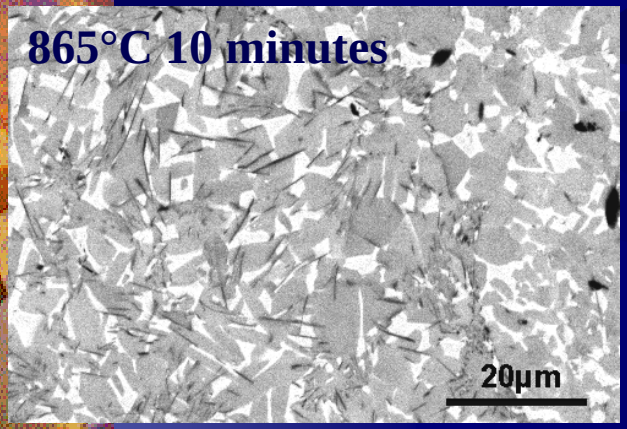

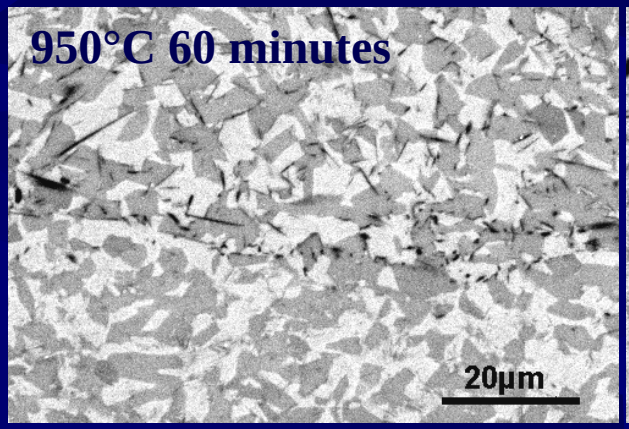

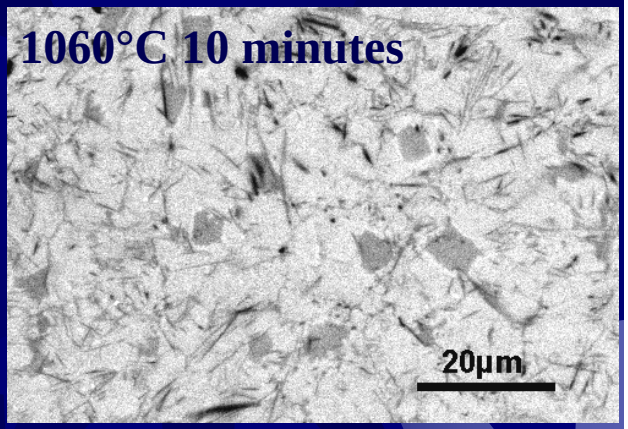

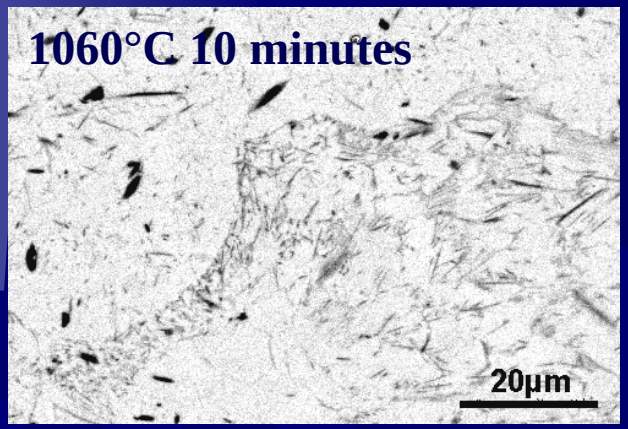

Increment of the beta transus temperature by the addition of B and C

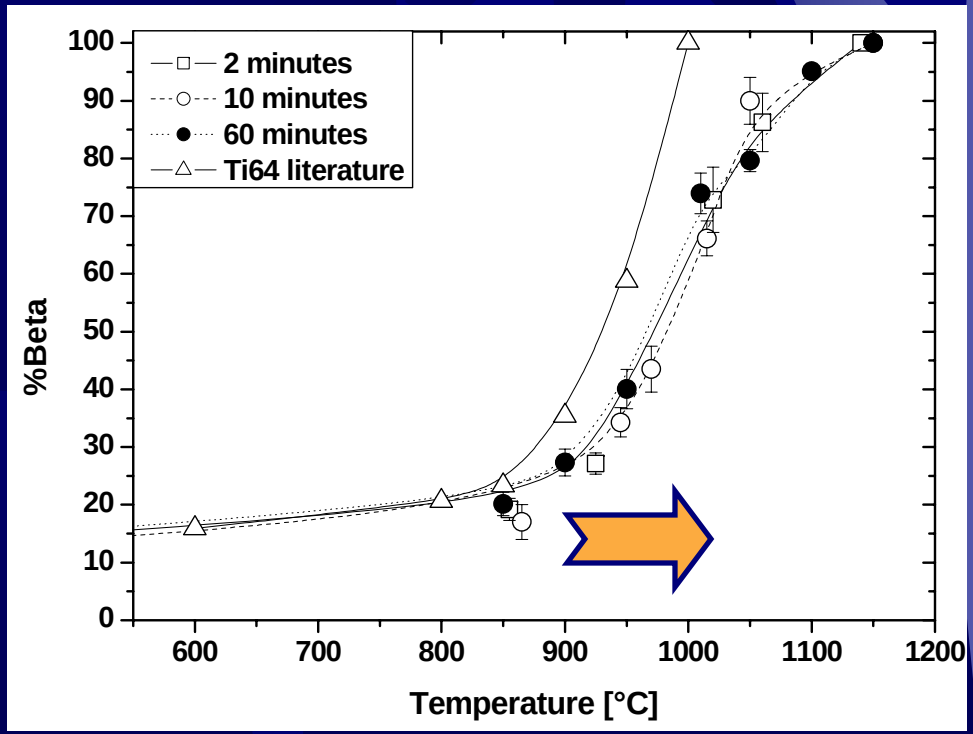

Results. Flow curves

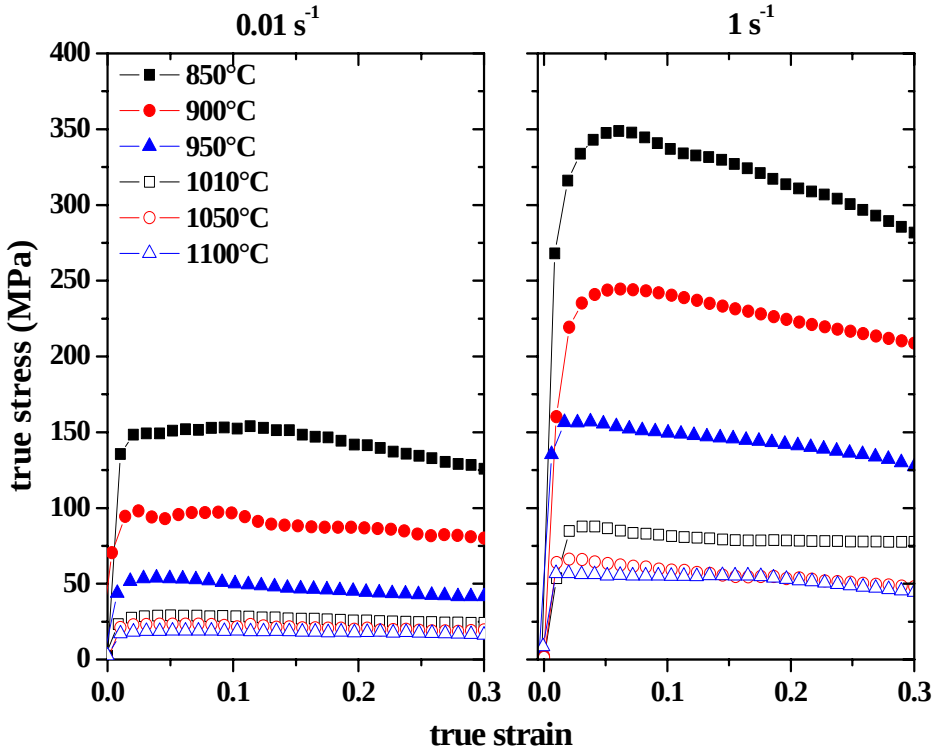

Ti64/TiB flow curves at 850-1100°C, 0.01 s^{-1} and 1s^{-1} Strong influence of the strain rate on the stress values

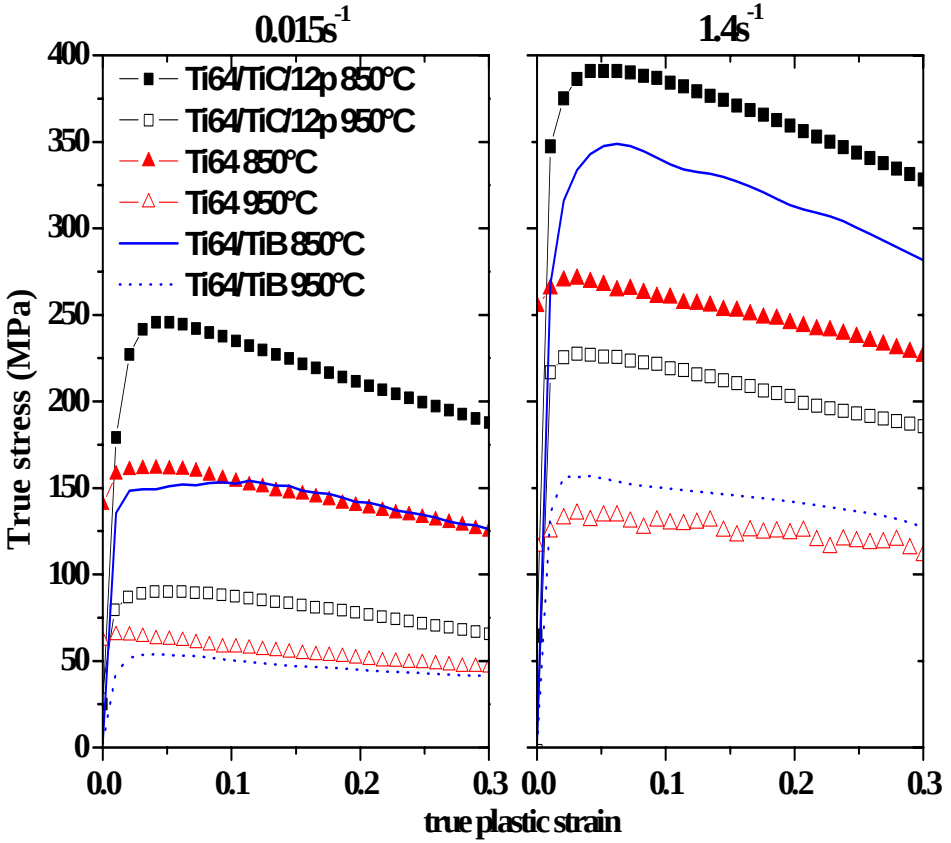

Flow curves at 850 and 950°C of Ti64/TiC/12p and Ti64 compared to Ti64/TiB at 0.015s^{-1} and 1.4s^{-1}. Similar softening but higher stress values for Ti64/TiC/12p.

Results. Deformation and damage

Ti64/TiB

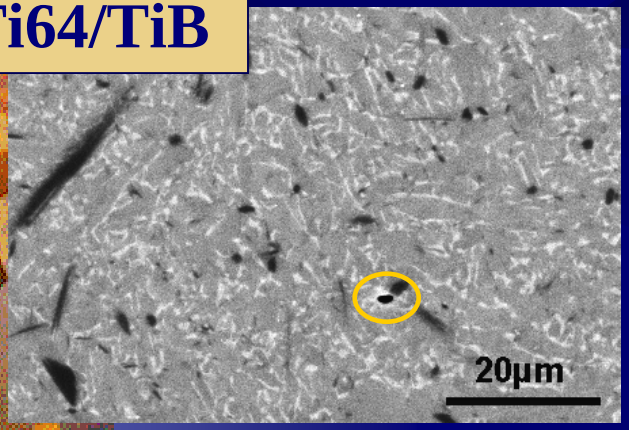

850°C 0.001s^{-1}: pores in the matrix

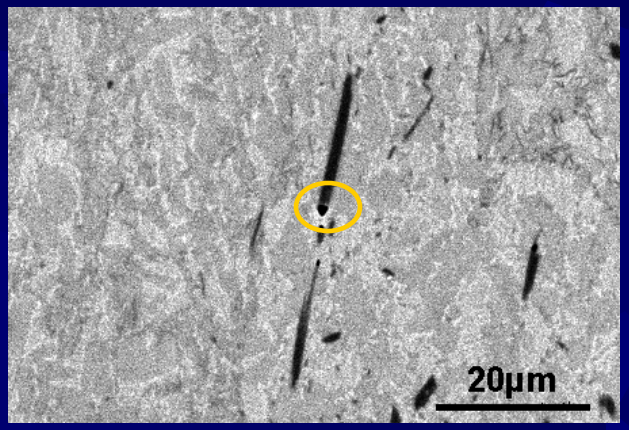

950°C 1s^{-1}: debonding of TiB

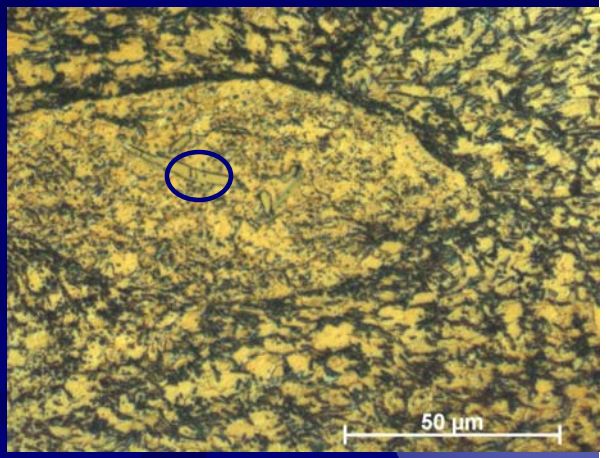

850°C 1s^{-1}: cracks in the TiB

Ti64/TiC/12p and Ti64

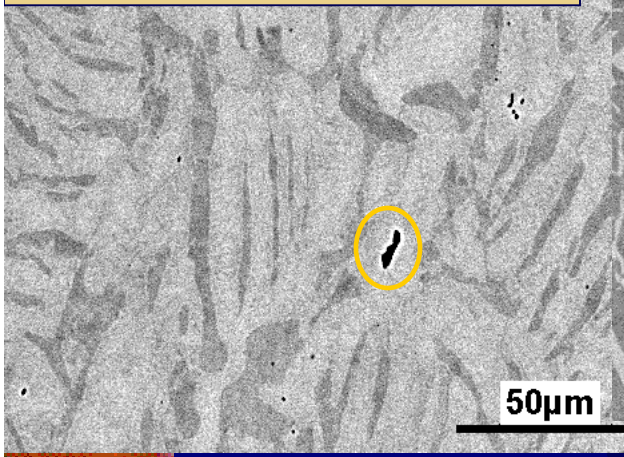

950°C 0.015s^{-1}: pores in β phase

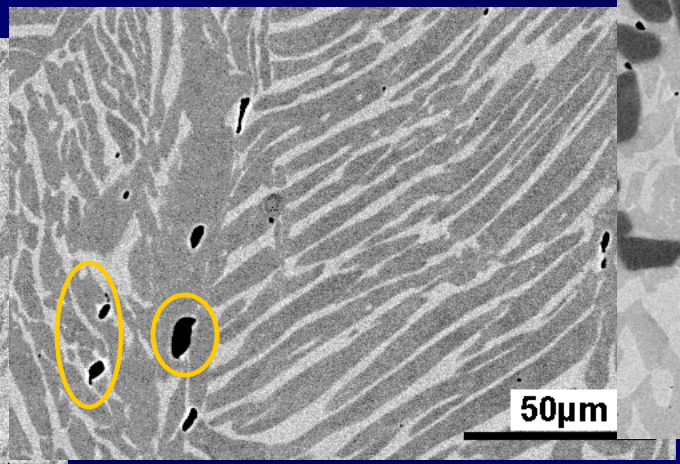

850°C 1.4s^{-1}: pores at the triple β prior grain boundary

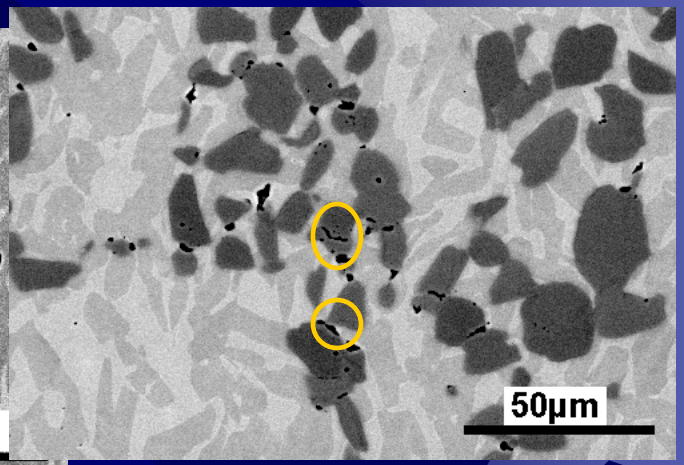

950°C 0.015s^{-1}: debonding of TiC particles

Discussion. Kinetic of deformation $\dot{\varepsilon} = K\sigma^n$

Two deformation behaviors for each temperature at 0.05 true strain

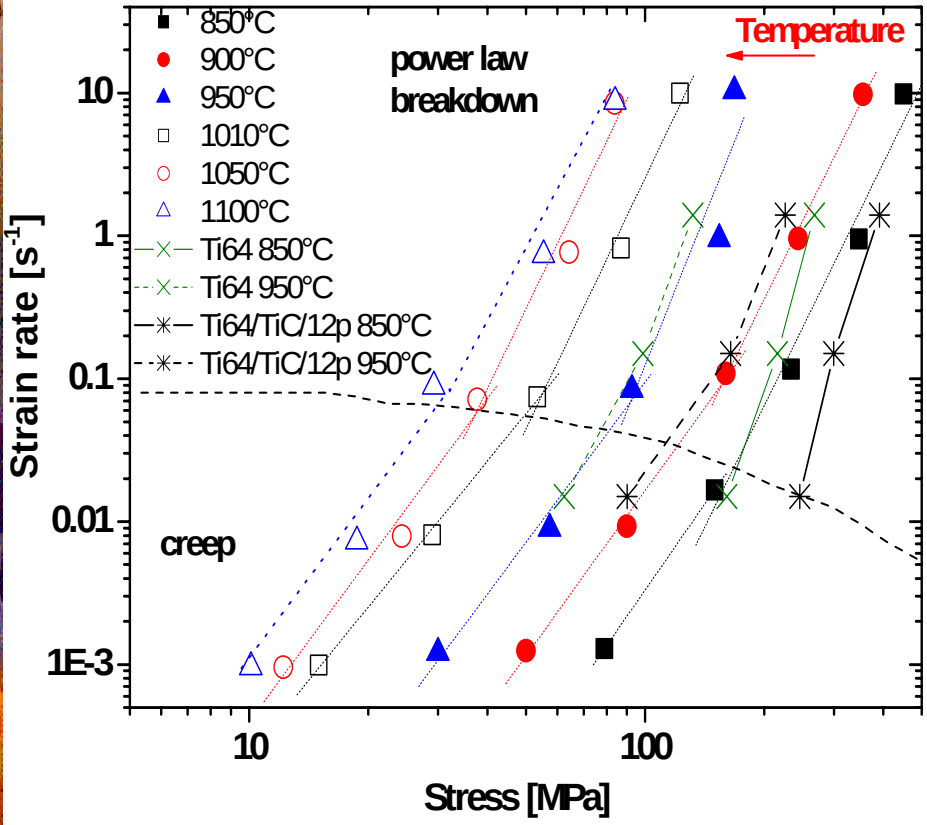

Ti64/TiB

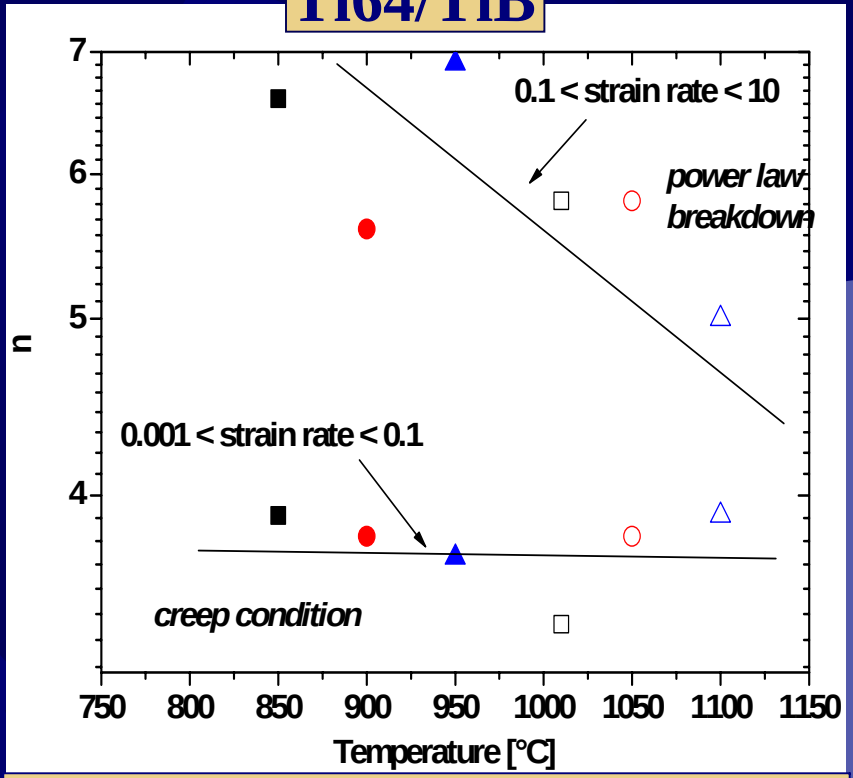

$0.1s^{-1} < \dot{\varepsilon} < 10s^{-1}$: n >4, decreases with increasing temperature. Power law breakdown.

$0.001s^{-1} < \dot{\varepsilon} < 0.1s^{-1}$: n ≈ 4 independent of temperature

Discussion. Kinetic of deformation

Ti64/TiB

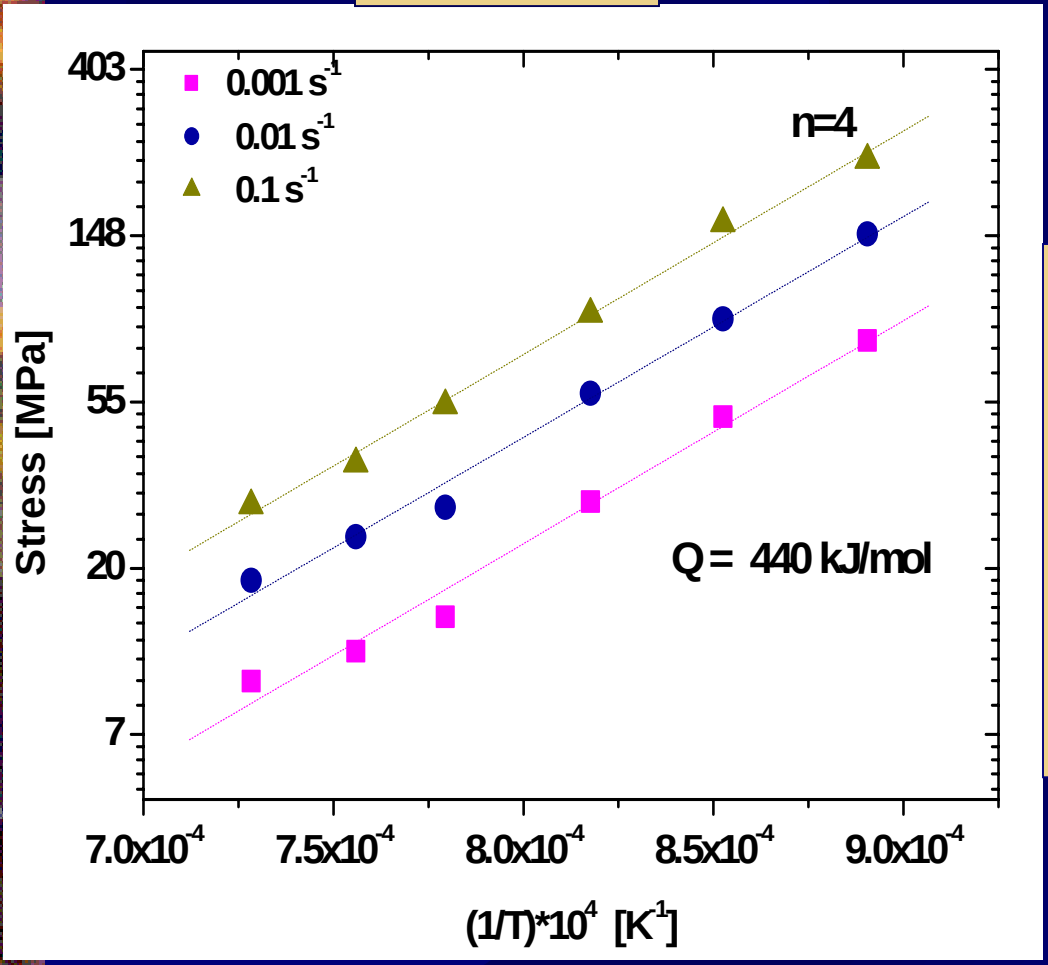

$$\dot{\varepsilon} = A\sigma^{n} e^{-Q/RT}$$

Q_{app} for Ti64/TiB ≈ 440kJ/mol, much higher than that for self diffusion in the α - phase (150kJ/mol), and higher than that for Ti64 equiaxed (330kJ/mol) in the α–β range due to the particle effect, and beta transus increase.

Conclusions

Increase of the β-transus by about 100°C with respect to Ti64 matrix for the composite reinforced with TiB.

Two mechanisms of hot compression found for Ti64/TiB:

- $0.001s^{-1} < \dot{\varepsilon} < 0.1s^{-1}$: thermally activated deformation mechanisms prevail yielding an exponent $n \approx 4$, with an apparent energy of diffusion ≈ 440kJ/mol.

$-0.1s^{-1} < \dot{\varepsilon} < 10s^{-1}$: power law breakdown, and dislocation mobility becomes more and more conservative. Small TiB whiskers act like dispersion strengthening .

-Strain hardening is counteracted by damage resulting in softening above 0.05 true strain.

- Damage in the Ti64 lamellar microstructure and in the TiC reinforced Ti64 enhanced due to higher strain concentrations compared to the fine globular microstructure of the Ti64/TiB composite.

Acknowledgments

-Dr. Mayer (Inst. of Materials Science and Technology.- Tech University Berlin) for the compression tests at high strain rates.

-The work is partially supported by the Federal Ministry of Economics and Labor in the framework of the Austrian Aeronautic Research (AAR) network

And thank you, for your attention!